Theoretical Investigation of the Photocatalysis Processes for Several Chlorinous Organic Compounds on the Anatase TiO₂ Surface using an Accelerated Quantum Chemical Molecular Dynamics Method

Chen Lv[1], Xiaojing Wang[1], Tomonori Kusagaya[1], Akira Endou[1],
Momoji Kubo[1,2], Akira Imamura[1,3] and Akira Miyamoto[1,4],*

[1]Department of Applied Chemistry, Graduate School of Engineering, Tohoku University,
Aoba-yama 07, Sendai 980-8579, Japan.
[2]PRESTO, Japan Science and Technology, 4-1-8 Honcho, Kawaguchi, Saitama 332-0012, Japan.
[3]Department of Mathematics, Faculty of Engineering, Hiroshima Kokusai Gakuin University,
6-20-1 Nakano, Aki-ku, Hiroshima 739-0312, Japan.
[4]New Industry Creation Hatchery Center, Tohoku University,Aoba-yama 10, Sendai 980-8579, Japan.
*Fax: +81-22-217-7235, Phone: +81-22-217-7233, e-mail: miyamoto@aki.che.tohoku.ac.jp

We have extended the application of our novel accelerated quantum chemical molecular dynamics program, 'Colors', which is more than 5000 times faster than the conventional first-principles quantum chemical molecular dynamics method, to the investigations of the photocatalytic processes for several chlorinous organic compounds (CH₃Cl and CHCl₃) on the anatase TiO₂ surface. The parameters for 'Colors' program were determined completely on the basis of the first-principles density functional calculations. The band gap energy of the anatase TiO₂ obtained by our method is in good agreement with the experimental result. The properties of the excited-state anatase TiO₂ were investigated and the adsorption and the photo-oxidation of CH₃Cl and CHCl₃ on the anatase TiO₂ surface were proposed.
Key words: Photo-oxidation, Titanium dioxide, Methyl chloride, Trichloromethane, Accelerated quantum chemical molecular dynamics method.

1. INTRODUCTION

The pollution of the water resources by sewage and industrial wastes is coming up as a serious problem recently. Chlorinous organic compounds in water cause not only the carcinogenic odor, but also the by-products of chemical reactions between pollutants and chlorine. The photocatalysis is one of the efficient ways to decompose these chloride compounds. Semiconductor materials as durable photocatalysts have been widely applied to such kind of environmental problems, with a special emphasize on the titanium dioxide (TiO₂). Of the three-polymorphic forms of TiO₂, viz., rutile, anatase and brookite, the anatase exhibits better photocatalytic properties with band gap energy of 3.2 eV. It has been used as effective sensitizers for light-reduced redox processes due to its electronic structure, which is characterized by a filled valence band and empty conduction band. Ultraviolet light or visible light is used to produce electron-hole pairs in TiO₂. Electrons react with oxygen to form O₂⁻ and holes react with surface hydroxyl groups to form OH· radicals. The radical species then attack the organic molecule, which is eventually oxidized to CO₂, H₂O and HCl if the organic molecule contains chlorine. However, the photocatalytic activities of anatase TiO₂ have not well been understood. Only a few investigations have been reported on the bulk properties. The band properties and structural constants have been provided by Pseudo-potential Hartree-Fock (PHF) calculations [1]. The orthogonalized linear combination of atomic-orbital method was also employed to calculate band structure.

In this work we have studied the photocatalytic behaviors of several important pollutants including methyl chloride (CH₃Cl) and trichloromethane (CHCl₃). A comprehensive study of the bulk and surface structure of the anatase TiO₂ has been done by density functional theory and our accelerated quantum chemical molecular dynamics methods. The optimized structure and binding energy of methyl chloride and trichlorimethane, as well as bulk anatase TiO₂ were derived. The density of state and excited state of molecular orbitals in the system were well analyzed and discussed. We have also reported the photo-adsorption processes of organic compounds on the anatase TiO₂ surface.

2. METHOD AND COMPUTAIONAL DETAILS

2.1 Density functional theory (DFT)

In this work, the density functional theory was used to investigate the properties of chloride organic compounds and crystalline TiO₂. The total energy, E, of the system is calculated in term of the following expression:

$$E = V_{NN} + H' + V_{ee} + E_{ex}(\rho) + E_{corr}(\rho) \quad (1)$$

where V_{NN} is the nuclear-nuclear interaction, H' is the mono-electronic contribution to total energy involving the kinetic energy of electrons and electron-nuclear interactions, V_{ee} is the Columbic

interaction between electrons, and $E_{ex}(\rho)$ and $E_{corr}(\rho)$ are the exchange and correlation energies, respectively. All terms except the nuclear-nuclear repulsion are the functions of the electron density ρ.

The optimized structure and electronic properties of CH₃Cl and CHCl₃ were calculated by Amsterdam Density Functional (ADF1999) [2] program. In ADF, the calculation was done by applying the triple-zeta basis sets containing a polarization functional with the Perdew-Wang (PW91XC) exchange and correlation potential function at the generalized gradient approximation (GGA) level [3]. The inner electrons within the core shells (1s for C; 2p for Cl) were frozen. The relativistic terms have been calibrated by a combined scalar relativistic zero order regular approximation (ZORA) [4]. The picture of the molecular orbital and optimized structure was illustrated using the MOLEKEL4.1 molecular visualization program [5]. The density of states for the crystalline TiO₂ was derived using the periodic methodology of Dmol³ program [6]. The double-numeric basis set with polarization functions (DNP) and the generalized gradient-corrected (GGA) functional, by Perdew, Burke, and Ernzerhof (PBE), were employed in this calculation. A Fermi smearing of 0.002 hartree and a real-space cutoff of 4 Å were used.

2.2 Accelerated quantum chemical molecular dynamics calculations

The understanding of the excited state and dynamical behavior are very important for the study of photocatalysis processes. Compared to small cluster models, large periodic models, which can represent the real properties, are useful to challenge these issues. However, current DFT method is not suitable to deal with large periodic models. In order to overcome the above problem, in the present study we developed a new accelerated quantum chemical molecular dynamics program 'Colors' [7-9], which is based on our original tight-binding approximation. We confirmed that our 'Colors' program with first principles parameterization can calculate the structure, and excited states of various molecules and large system of solid as accurately as the density functional calculations, while the CPU time of the new method is around 5,000 times faster than that of the first-principles molecular dynamics calculations. In "Colors", the total energy, E is expressed by Eqs. (2).

$$E = \sum_{i=1}^{N}\frac{1}{2}m_i v_i^2 + \sum_{k=1}^{OCC}\varepsilon_k + \sum_{i=1}^{N}\sum_{j>i}^{N}\frac{Z_iZ_je^2}{r_{ij}} + \sum_{i=1}^{N}\sum_{j>i}^{N}E_{repuls}(r_{ij})\,(2)$$

In Eq. (2) the first, second, third, and fourth terms represent the kinetic energy, the summation of the eignvalues for all occupied orbitals (orbital energy of valence electrons), the Coulombic interaction energy, and the short-range exchange-repulsion energy, respectively. Furthermore, the short-range exchange-repulsion

term E_{repuls} is represented as follows:

$$E_{repuls}(r_{ij}) = b_{ij}\exp\left(\frac{a_{ij}-r_{ij}}{b_{ij}}\right)\qquad(3)$$

The corrected distance-dependent expression K for off-diagonal terms of the Hamiltonian H_{rs} is employed:

$$H_{rs} = \frac{1}{2}K_{rs}(H_{rr}+H_{ss})S_{rs}\qquad(4)$$

$$K = 1+(k_{rs}+\Delta^2-\Delta^4 k_{rs})\exp[-\delta_{rs}(R_{ij}-d_0)]\,(5)$$

$$\Delta = (H_{rr}-H_{ss})/(H_{rr}+H_{ss})\qquad(6)$$

where d_0 is the sum of the orbital radii. We employed parameters such as the Slater exponent and the valence state ionization potential (VISP) of each atomic orbital for the acceleration. The diagonal Hamiltonian, H_{rr}, is set up equal to the ionization energy of each atomic orbital. The parameters K_{rs} and δ_{rs} come from the chemical bonding calculations. Moreover, In "Colors" the force is expressed by Eqs. (7)

$$F_i = \sum_{j\neq i}^{N}\sum_{k=1}^{OCC}C_k^T\frac{\partial H}{\partial r_{ij}}C_k + \sum_{j\neq i}^{N}\sum_{k=1}^{OCC}\varepsilon_k C_k^T\frac{\partial S}{\partial r_{ij}}C_k -$$
$$\sum_{j\neq i}^{N}\frac{Z_iZ_je^2}{r_{ij}^2} + \sum_{j\neq i}^{N}\frac{\partial E_{repuls}(r_{ij})}{\partial r_{ij}}\qquad(7)$$

In order to increase the accuracy, the parameters were determined by our new parameterization procedure based on the first-principles density functional theory calculations. The optimized structure and molecular obitals were visualized using New-RYUGA software developed in our laboratory [10].

3. RESULTS AND DISCUSSION

3.1. Optimized structure and molecular orbitals of CH₃Cl and CHCl₃

The fully optimized structures of CH₃Cl and CHCl₃ were obtained by minimizing the total energy and atomic force by 'Colors' and ADF1999 programs. The total energy of the CH₃Cl molecule was −22.098 eV and −22.303 eV by 'Colors' and ADF programs, respectively, while that of the CHCl₃ molecule was −18.638 eV and −18.649 eV by 'Colors' and ADF programs, respectively. These results show that the 'Colors' program well reproduces the density functional theory calculation results. The optimized structural parameters by 'Colors' program are also in good agreement with the ADF and experimental results.

The qualitative sketch of the highest occupied molecular orbital (HOMO) and lowest unoccupied molecular orbital (LUMO) obtained by the ADF and 'Colors' programs are given in Fig. 1. Both results show that HOMO of CH₃Cl is from the orbital of Cl-3p$_z$, and LUMO of CH₃Cl is an anti-bonding (σ^*) combination of the C-2p$_x$ and Cl-3p$_x$, while HOMO of CHCl₃ is the mixing of Cl-3p$_z$ and Cl-3p$_y$ and LUMO of CHCl₃ is a

orbital mixed by Cl-$3p_x$ and Cl-$3p_y$. Since the calculation results by 'Colors' program well reproduces the density functional theory calculation results, we confirmed the accuracy of our 'Colors' program.

3.2. Optimized structure and electronic properties of anatase TiO_2

Fig. 2 depicts the unit cell of the anatase TiO_2 structure, which was calculated by 'Colors' program under the periodic boundary conditions. Calculated two lattice parameters, a and c, by 'Colors' program as shown in Table 1, are well consistent with first-principle calculations using the full-potential linearized augmented plave-wave method (FLAPW) [11] and the experimental data [12].

The density of states (DOS) for the anatase TiO_2 calculated by 'Colors' program is presented in Fig. 3. The top state of valence band (VB), between -16.75 eV and -8.47 eV, is mainly made up by O 2p orbitals and has a small contribution of Ti 3d orbitals. The beginning part of conduction bands (CB) is consisted by Ti 3d. It suggests that there is a substantial degree of hybrid between O 2p and Ti 3d in both VB and CB regions, that is, the strong interaction exists between Ti and O atoms in the anatase TiO_2. The band gap energy of 2.0 eV was obtained by Asahi et al. using the FLAPW method [11]. However, it is much smaller than the experimental value of 3.2 eV. Thus in this work we performed the 'Colors' calculation of the band gap energy. Obviously it can be found from Fig. 3, a band gap of 3.15 eV, obtained by our 'Colors' program, is very close to the experimental one (3.2 eV) [13].

Furthermore, the binding energy of the anatase TiO_2 is derived using 'Colors' and $Dmol^3$ programs. They gave the consistent results that is -353.09 eV by 'Colors' and -353.2 eV by $Dmol^3$. All these results indicate that the geometries and electronic properties of the anatase TiO_2 can be reproduced very well and confirm the reliability of our 'Colors' program.

3.3 The processes of photo-oxidation of CH_3Cl and $CHCl_3$ on anatase TiO_2 surface

The (110) surface of the anatase TiO_2 was chosen in this work because it is well-known that (110) surface is most stable surface. On the well characterized an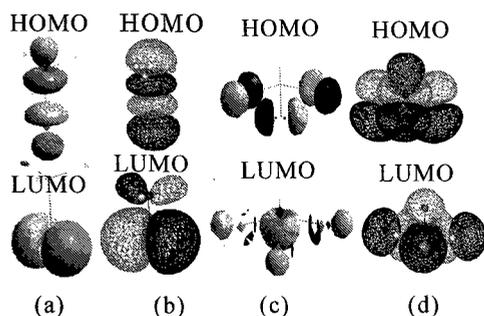atase TiO_2 (110) surface, one can accurately measure and control the coverage of surface defects, adsorbed molecular oxygen, surface hydroxyl groups, and adsorbed CH_3Cl and $CHCl_3$. Fig. 4(a) depicts the CH_3Cl adsorbed on the TiO_2 (110) surface completely covered with dissociated water. Fig. 4(b) depicts the CH_3Cl adsorbed on the TiO_2 (110) surface covered with dissociated water and oxygen. Fig. 4 (c) and (d) depicts the $CHCl_3$ adsorbed on the TiO_2 (110) surface covered with dissociated water and oxygen, respectively. Four kinds of models were calculated by 'Colors' program. The HOMO and LUMO of the excited-state of the TiO_2 surface are obtained for each model. Figs. 5 and 6 show the transfer of electron from the HOMO of the excited anatase TiO_2 (110) surface to the LUMO of CH_3Cl and $CHCl_3$, respectively. From these figures, it can be found easily that the electron transfer in the case of (b) is easier than that in the case of (a). Moreover, in the case of (d) the electron transfer is easier than that in the case of (c). Our results clearly demonstrate that oxygen molecules adsorbed at surface are essential conditions for the photo-oxidation reaction in the initiate state as well as in the proceeding.

The energy levels of these frontier molecular orbitals are depicted in Fig. 7. It can be seen that the difference between the HOMO of the exited-state of the anatase TiO_2 in Fig. 4 (b) and the LUMO of the ground-state of $CHCl_3$ is about 1.45 eV, while the difference between the HOMO of the excited-state of the antase TiO_2 in Fig. 4 (d) to the LUMO of the ground-state of CH_3Cl is about 2.9 eV. Therefore it can be concluded that $CHCl_3$ is more oxidizable than CH_3Cl.

Table 1 Lattice parameters for anatase TiO_2 obtained by 'Colors' program, FLAPW calculation, and experiments.

	Colors	FLAPW[11]	Exp. [12]
a(Å)	3.770	3.692	3.872
c(Å)	9.481	9.471	9.502

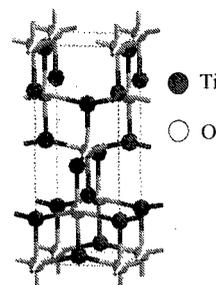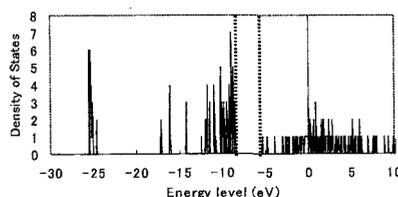
Fig.2 Structure of the anatase TiO_2.

Fig. 3 Total density of state (DOS) of antase TiO_2. The left dashed line indicates the maximum value of conduction band, while the right dashed line indicates the minimum value of valence band.
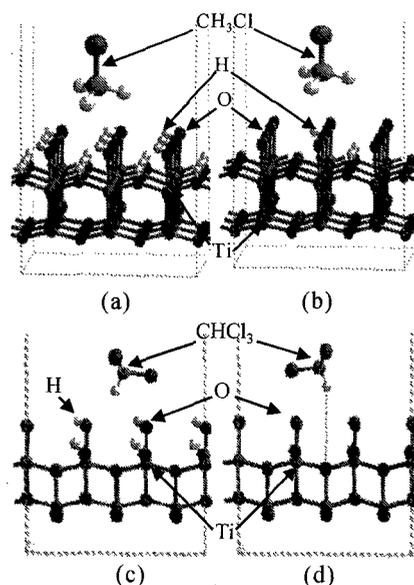

(a)　　　(b)　　　(c)　　　(d)

Fig. 1 HOMO and LUMO of CH_3Cl and $CHCl_3$. (a) ADF results of CH_3Cl, (b) Colors results of CH_3Cl, (c) ADF results of $CHCl_3$, and (d) Colors results of $CHCl_3$. The top part represents HOMO. The bottom part represents LUMO.

Fig.4 CH₃Cl and CHCl₃ adsorbed on the anatase TiO₂(110) surface. (a) CH₃Cl on the TiO₂ surface covered with dissociated water, (b) CH₃Cl on the TiO₂ surface covered with dissociated water and oxygen, (c) CHCl₃ on the TiO₂ surface covered with dissociated water, (d) CHCl₃ on the TiO₂ surface covered with oxygen.
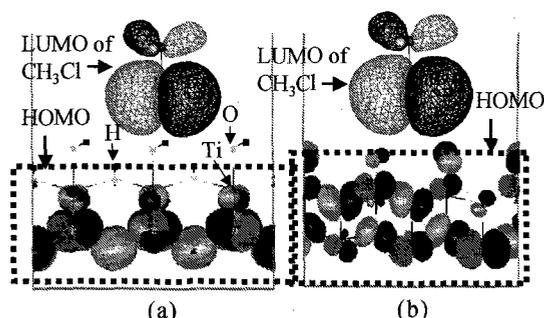

Fig. 5 (a) LUMO of the ground-state of CH₃Cl and HOMO of the excited-state of the TiO₂ covered with dissociated water and (b) LUMO of ground-state of CH₃Cl and HOMO of excited-state of TiO₂ covered with dissociated water and oxygen.
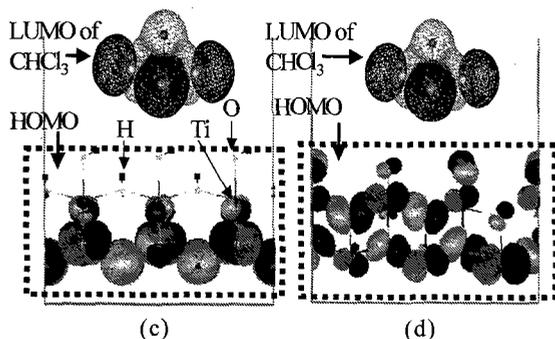

Fig. 6 (c) LUMO of the ground-state of CHCl₃ and HOMO of excited-state of the TiO₂ covered by dissociated water (d) LUMO of the ground-state of CHCl₃ and HOMO of excited-state of the TiO₂ covered with dissociated water and oxygen.

4. CONCLUSIONS

This work has investigated fully optimized structures and electronic properties of organic compounds CH₃Cl and CHCl₃ as well as anatase TiO₂ by 'Colors' program and density functional theory method. The nature of the main electronic features of the anatase TiO₂ was interpreted on the basis of density of states of molecular orbitals. The adsorption and the photo-oxidation processes of CH₃Cl and CHCl₃ on anatase TiO₂ surface was proposed by analyzing the energy levels of molecular orbitals reasonably.

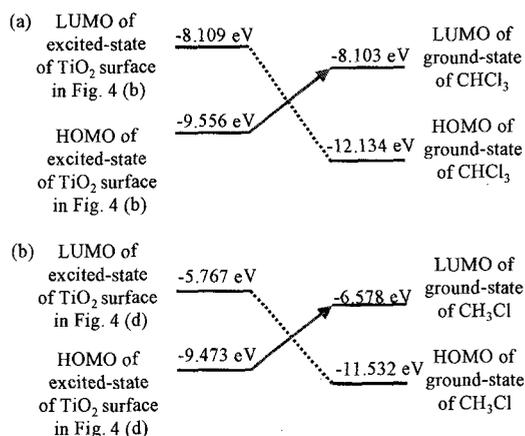Fig. 7 The energy levels of molecular orbitals. (a) HOMO and LUMO energy levels of TiO₂ surface in Fig. 4(b) and CHCl₃, (b) The HOMO and LUMO energy levels of TiO₂ surface in Fig. 4(d) and CH₃Cl

REFERENCES

[1] A. Fahmi, C. Minot, B. Silvi, and M. Causa, *Phys. Rev. B*, **51**, 13023 (1995).
[2] F. C. Guerra, J. G. Snijders, B. Velde, and, E. J. Baerends, *Theor. Chem. Acc.*, **99**, 391 (1998).
[3] J. P. Perdew, J. A. Chevary, S. H. Vosko, K. A. Jackson, M. R. Pederson, and, D. J. Singh, *Phys. Rev. A*, **46**, 6671 (1992).
[4] E. V. Lenthe, A. E. Ehlers, and E. J. Baerends, *J. Chem. Phys.*, **110**, 8943 (1999).
[5] S. Portmann and H. P. Luthi, *Chimia*, **54**, 766 (2000).
[6] B. Delley, *J. Chem. Phys.*, **92**, 508 (1990).
[7] T. Yokosuka, K. Sasata, H. Kurokawa, S. Takami, M. Kubo, A. Imamura, Y. Kitahara, M. Kanoh, and, A. Miyamoto, *Jpn. J. Appl. Phys.*, **42**, 1877 (2003).
[8] K. Sasata, T. Yokosuka, H. Kurokawa, S. Takami, M. Kubo, A. Imamura, T. Shinmura, M. Kanoh, P. Selvam, and A. Miyamoto, *Jpn. J. Appl. Phys.*, **42**, 1859 (2003).
[9] M. Elanany, P. Selvam, T. Yokosuka, S. Takami, M. Kubo, A. Imamura, and A. Miyamoto, *J. Phys. Chem. B*, **107**, 1518 (2003).
[10] R. Miura, H. Yamano, R. Yamauchi, M. Katagiri, M. Kubo, R. Vertrivel, and A. Miyamoto, *Catal. Today*, **23**, 409 (1995).
[11] R. Asahi, Y. Taga, W. Mannstadt, and, A. J. Freeman, *Phys. Rev. B*, **61**, 7459 (1999).
[12] J. K. Burdett, T. Hughbanks, G. J. Miller, J. W. Richardson, Jr., and, J. V. Smith, *J. Am. Chem. Soc.*, **109**, 3639 (1987).
[13] H. Tang, H. Berger, P. E. Schmid, F. Levy, and G. Burri, *Solid State Comm.*, **23**, 161 (1977).